

MODELING AND QUANTIFICATION OF ACOUSTIC DAMPING INDUCED BY VORTEX SHEDDING IN NON-COMPACT THERMOACOUSTIC SYSTEMS

Tobias Hummel^{1,2}, Thomas Hofmeister¹, Bruno Schuermans^{2,3}, Thomas Sattelmayer¹

¹*Lehrstuhl für Thermodynamik, Technische Universität München, Germany*

²*Institute for Advanced Study, Technische Universität München, Germany*

³*GE Power, Switzerland*

EMAIL: hummel@td.mw.tum.de

This paper presents a methodology to compute acoustic damping rates of transversal modes due to vortex-shedding. This acoustic damping rate presents one key quantity for the assessment of linear thermoacoustic stability of gas turbine combustors in the high-frequency regime. State-of-the-art network models – as employed to calculate damping rates in low-frequency, longitudinal systems – cannot fulfill this task due to the acoustic non-compactness encountered in the high-frequency regime. Furthermore, direct eigensolutions of the Linearized Euler Equations (LEE) yield incorrect results for the damping rates due to the implicit presence of acoustic as well as hydrodynamics contributions in these solutions. The proposed methodology consist of three steps: (1) The regions in which acoustic fluctuations are transformed into vortical disturbances are identified from LEE simulation results. (2) The respective regions are modeled as acoustic momentum sinks, which are suitably included in the Helmholtz Equation (HE). (3) The unknown loss coefficients are obtained by requiring equality between reflection coefficients (which is a purely acoustic quantity) of the concerned configuration obtained from LEE and HE plus sink model. The desired acoustic damping rates are then computed by solving the respective HE for the transversal eigenmodes of interest. The methodology's applicability to technically relevant systems is demonstrated by a validation test case using a lab-scale, swirl-stabilized combustion system.

Introduction

Thermoacoustic instabilities are detrimental to lean-premixed combustion systems. Their avoidance presents a predominant challenge for design and operation of modern gas turbines for power generation. These instabilities are understood as the consequence of Rayleigh's criterion, which states that acoustic energy is generated at a particular eigenmode of the combustor when oscillations of the flame's heat release rate and fluid pressure are in-phase. Such oscillations of heat release are caused by naturally present acoustic (eigen-)oscillations, which penetrate/disturb the combustion process. Thus, a mutual amplification of heat release and acoustic oscillations takes place, and establishes a constructive feedback between the former and the latter. If the acoustic dissipation is lower than the generated energy, the acoustic oscillations receive a net supply of energy. This energy supply initiates a growth in oscillation amplitude until saturated by non-linear mechanisms associated with the flame dynamics. Once the dissipated energy equates the supplied energy, a constant amplitude limit cycle state establishes at a particular eigenmode/-frequency. Hence, one decisive factor whether an instability occurs is the strength of acoustic dissipation at the concerned eigenmodes of the system, which presents the central subject of this work. One physical mechanism that leads to acoustic dissipation is the interaction between the acoustic oscillations and shear-layers of the flow, as e.g. found in free or swirling jet streams. This process induces periodic formations of coherent flow vortices that can be interpreted as a sink of acoustic energy, i.e. acoustic damping. Such periodic vortex formations are shown in Fig. 1 a) via Mie-Scattering images [1] that are triggered by the first transversal mode in the outer shear layer of a swirling velocity field in an experimental combustor. Notice that this combustor experiment (cf. [1] and [2] for details) serves as the validation test case

in this work. Associated, numerically obtained fields of axial mean velocity and instantaneous velocity disturbances from numerical simulations are illustrated in Figs. 1 b)-c). The corresponding dissipation of acoustic power is visualized through Howe's equation (cf. [3] and details below) in Fig. 1 d). Other damping mechanisms (not considered in this work) are the formation of entropy disturbances due to interactions between acoustics and mean flow temperature gradients and dissipation in the acoustic boundary layer [4].

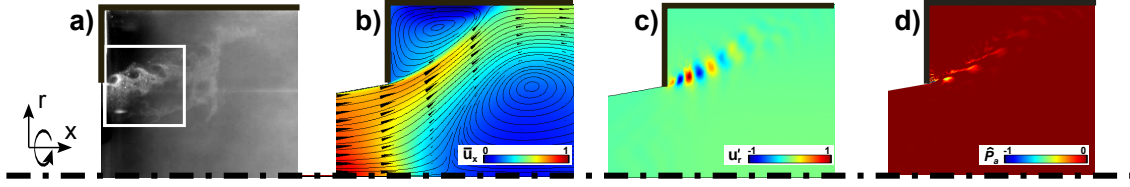


Figure 1: a) Mie scattering of period vortex-shedding [1], b) Normalized mean velocity field, c) Normalized instantaneous velocity disturbance field, d) Normalized acoustic power dissipation

One approach for mitigating the occurrence of thermoacoustic oscillations is to pursue a design-for-stability strategy, which implies the computational assessment of the linear stability for new combustor designs, for modifications of existing combustors via retrofits or implementation of stability enhancement devices. For this purpose, low-order linear stability tools have been readily developed and applied. These tools are typically based on a modal approach, which implies that the thermoacoustic oscillations are governed by a complex Fourier series, i.e.

$$\phi'(\mathbf{x}, t) = \text{Real} \left(\sum_{n=0}^N \hat{\phi}(\mathbf{x}, \omega_n) \exp(i\omega_n t) \right). \quad (1)$$

In Eqn. 1, ϕ represents the spatially dependent (\mathbf{x}) acoustic variable (i.e. pressure p , vectorial velocity \mathbf{u} and density ρ). The prime (') denotes oscillations in time (t), while the system's eigenmodes – which constitute the summation expansions – are complex amplitude distributions, which are indicated by the hat (^). Having included all energy addition and removal processes (i.e. flame driving and acoustic dissipation) in the stability tools, yields the complex eigenfrequency, i.e.

$$\omega_n = 2\pi f_n - i\alpha_{n,a} \quad (2)$$

where f_n is the oscillation frequency, $\alpha_{n,a}$ is the acoustic growth rate, and the subscript a indicates a strict correspondence to acoustic quantities. The value of the growth rate essentially defines the linear stability state of mode n , and thus of the thermoacoustic system:

$$\alpha_{n,a} > 0 \rightarrow \text{unstable} \quad (3)$$

$$\alpha_{n,a} < 0 \rightarrow \text{stable} \quad (4)$$

Interpretatively, the growth rates describe the normalized change of oscillation energy, which gives by definition

$$\alpha_{n,a} \propto \frac{1}{E_{n,a}} \frac{dE_{n,a}}{dt} = \text{const.} \quad (5)$$

where $E_{n,a}$ can be interpreted as the period-averaged net energy amount due to acoustic driving and damping mechanisms. An important physical/mathematical feature of acoustic oscillations associated with Eqn. 5 is the potential flow nature of the associated fluid motions, i.e. the irrotationality of the acoustic velocity field $\nabla \times \hat{\mathbf{u}} = 0$. The growth rate can be decomposed into

$$\alpha_n = \alpha_{n,a,\text{flame}} + \alpha_{n,a,\text{flow}} \quad (6)$$

where $\alpha_{n,a,\text{flame}} > 0$ and $\alpha_{n,a,\text{flow}} < 0$ are the acoustic driving rate and damping rate caused by interactions with the flame and flow's shear layer at mode n , respectively. Notice that in theory, the opposite situation can prevail too, i.e. damping by the flame and driving by the shear layer [5], which is disregarded in this paper for clarity reasons.

Referring to Eqns. 3-4 and 6, if driving exceeds damping, an instability impends, and vice versa. Thus, the

task of stability assessment comes down to correctly including all energetic contribution in the respective computational model of the concerned combustion system. Low-frequency (i.e. below the concerned chambers cut on frequency) oscillations are constituted by longitudinal, one-dimensional mode shapes. Flame driving and acoustic damping occur in an acoustically compact/zero-dimensional manner, which implies that the associated wave-lengths are larger than the respective interaction zones (e.g. combustion and shear layer regions). In terms of modeling, these interactions are included by zero-dimensional transfer functions (analytically, numerically, or experimentally obtained) in well established network modeling approaches ([6]).

For high-frequency instabilities – which have become an increasingly relevant challenge in industrial gas turbine combustors [7] – the compactness assumption no longer prevails, and thus, restricts the application of network models. This is due to the governance of the oscillations by multi-dimensional mode shapes at frequencies above the chamber's cut on value. Associated wave lengths are small, which leads to a spatial variability of flame driving and acoustic dissipation mechanisms across the corresponding combustion and shear layer regions. Hence, high-frequency instabilities are synonymously referred to as non-compact thermoacoustic oscillations. In order to model a non-compact system's thermoacoustic stability, spatially varying/non-compact transfer functions are required. For the driving part, details on analytical modeling and experimental obtainment of non-compact transfer functions are readily provided in previous work of the authors in [8]. An analogous treatment of acoustic damping have seemingly not yet been pursued, but is crucially needed for a complete linear stability assessment of non-compact systems. In this work, a methodology is proposed with which the acoustic damping of transversal modes due to shear-layer interactions can be modeled and quantified by a local transfer function.

The paper is structured as follows: The first section provides relevant theoretical background and states the research objectives. The second section presents the modeling methodology along with the analysis procedure. Then, a respective verification and validation test case is carried out in section three. The test case results are shown and discussed in the forth section before the paper is concluded.

1. Theoretical Background and Problem Statement

This section establishes governing equations, presents the research objectives, and proposed the associated modeling methodology to achieve those objectives.

1.1 Governing Equations

Unsteady/oscillatory flow problems that are characterized by small disturbances from a spatially non-uniform steady state are governed by the Linearized Euler Equations (LEE) in frequency domain:

$$\bar{\rho} (i\omega \hat{\mathbf{u}} + \bar{\mathbf{u}} \cdot \nabla \hat{\mathbf{u}} + \hat{\mathbf{u}} \cdot \nabla \bar{\mathbf{u}}) + \hat{\rho} \bar{\mathbf{u}} \cdot \nabla \bar{\mathbf{u}} + \nabla \hat{p} = \hat{\mathbf{F}}_{\hat{\mathbf{u}}}, \quad (7)$$

$$i\omega \hat{p} + \bar{\mathbf{u}} \cdot \nabla \hat{p} + \hat{\mathbf{u}} \cdot \nabla \bar{p} + \gamma \bar{p} \nabla \cdot \hat{\mathbf{u}} + \gamma \hat{p} \nabla \cdot \bar{\mathbf{u}} = \hat{F}_{\hat{p}}. \quad (8)$$

In these equations, the steady mean flow (bar symbol ($\bar{}$)) includes velocity, pressure as well as density. This mean flow field is obtained e.g. by numerical simulations. The solution variables (hat symbol ($\hat{}$)) are the complex amplitude distributions/mode shapes of the disturbed flow variables at an associated angular frequency ω . Note that the disturbances of density and pressure are related through the speed of sound by $\rho(\mathbf{x})\bar{c}(\mathbf{x})^2 = \hat{p}(\mathbf{x})$ in Eqns. 7-8, which implies the assumption that the flow disturbances behave isentropically. The mode shapes may either correspond to (complex) eigenfrequencies of the system or to (real) prescribed values as a response to external excitation. The right hand sides of Eqns. 7-8 host respective volumetric terms $\hat{\mathbf{F}}_{\hat{\mathbf{u}}}$ and $\hat{F}_{\hat{p}}$. Maintaining a three dimensional dependency of the solution variables and source terms automatically accounts for any thermoacoustical non-compactness associated with transversal acoustic modes. The LEE mathematically capture all linear interactions between shear layer and flow disturbance, i.e. the acoustic triggering of periodic vortex-shedding. This process represents a transformation of acoustic (sink) into vortical disturbances (source) at the location of the interactions. Consequently, solutions of Eqns. 7-8 contain acoustic as well as vortical disturbances that respectively propagate with the speed of sound and the mean flow velocity in a superposed manner (cf. further details in the next subsection).

Numerical solutions (eigenmodes/-frequencies or forced modes at predefined frequencies) can be obtained using a stabilized Finite Element Method (sFEM). The stabilization is required in order to avoid spurious solutions

caused by the convective terms of the LEE [9]. The residual based Streamline Upwind Petrov Galerkin (SUPG) artificial diffusion scheme is employed for this work, which yields to following discrete form of Eqns. 7-8:

$$i\omega \mathbf{E} \hat{\phi} = (\mathbf{A} + \tau \mathbf{A}_{SUPG}) \hat{\phi} + \mathbf{B} \quad (9)$$

In this expression, \mathbf{E} , \mathbf{A} and \mathbf{A}_{SUPG} denote discretization matrices associated with the time derivatives (i.e. $i\omega$ terms), spatial derivatives and SUPG stabilization operators, respectively. The solution vector $\hat{\phi} = (\hat{p} \ \hat{\mathbf{u}})^T$ hosts the solution variable at every node in the mesh, while the source term vector \mathbf{B} remains unspecified at this point. The constant parameter τ allows to the control numerical stabilization strength and is specified by the user. Note that all necessary boundary conditions to compute a problem-specific solutions (cf. details further below) are assumed as already included in Eqn. 9.

At this point, the question arises how to obtain the desired acoustic damping rate $\alpha_{n,a}$ at the mode of interest due to vortex shedding. It is intuitive to presume that simply solving Eqn. 9 for the complex eigenfrequency would yield this damping rate. Unfortunately, as is explained in the following, this would yield incorrect results and compromise the reliability/correctness of the entire stability assessment.

1.2 Research Objectives

The reason why direct eigensolutions of the LEE cannot be used for the quantification of pure acoustic damping is of physical origin. As mentioned before, the vortex-shedding processes governed by Eqns. 7-8 include acoustic and vortical disturbances that compose the unsteady fluid velocity, i.e.

$$\hat{\mathbf{u}} = \hat{\mathbf{u}}_a + \hat{\mathbf{u}}_v, \quad (10)$$

where the former and latter vector fields are irrotational ($\nabla \times \hat{\mathbf{u}}_a = 0$) and solenoidal ($\nabla \cdot \hat{\mathbf{u}}_v = 0$), respectively. The normalized change of periodically averaged energy (as in Eqn. 5) associated with an LEE eigenmode can be explicitly formulated (cf. [5]), and is given by

$$\alpha_n \propto \frac{1}{E_n} \frac{dE_n}{dt} \propto \frac{\left| \int_V \bar{\rho} \bar{\mathbf{u}} \cdot (\hat{\bar{\boldsymbol{\Omega}}} \times \hat{\mathbf{u}}) + \hat{\rho} \hat{\mathbf{u}} \cdot (\bar{\boldsymbol{\Omega}} \times \bar{\mathbf{u}}) dV \right|^2}{\left| \int_V \hat{p}^2 / \bar{\rho} + \bar{\rho} (\hat{\mathbf{u}} \cdot \hat{\mathbf{u}}) + 2 \hat{\rho} \bar{\mathbf{u}} \cdot \hat{\mathbf{u}} dV \right|^2}, \quad (11)$$

where α_n represents the imaginary part, i.e. damping rate, of the eigenfrequency in Eqn. 9, $\bar{\boldsymbol{\Omega}} = \nabla \times \bar{\mathbf{u}}$, and $\hat{\bar{\boldsymbol{\Omega}}} = \nabla \times \hat{\mathbf{u}}$ are mean and disturbed flow vorticity, respectively. From Eqns. 10 and 11 it follows that

$$\frac{1}{E_n} \frac{dE_n}{dt} = \frac{1}{E_{a,n}} \frac{dE_{a,n}}{dt} + \frac{1}{E_{v,n}} \frac{dE_{v,n}}{dt} \rightarrow \alpha_n = \alpha_{n,a} + \alpha_{n,v}. \quad (12)$$

Equation 12 reveals that damping rates obtained from LEE eigensolutions indeed contain pure acoustic contributions, but also vortical contributions. For this work, the former quantitatively describes the loss of acoustic oscillation energy due to vortex shedding, while the latter contains all energy conversion processes associated with the vortical disturbances [3]. However, it is crucial to point out that the assessment of thermoacoustic stability in accordance with Eqns. 3-4 and 6 requires the pure acoustic damping rate $\alpha_{a,n}$, which is associated with the irrotational disturbance field $\hat{\mathbf{u}}_a$. Hence, any direct use of LEE damping rates for thermoacoustic stability assessment is physically and theoretically prohibited. A separation of the potential and vortical components of Eqn. 10 – and thus of Eqn. 11 – is not straight-forwardly possible. Hence, a methodology is needed that allows to quantify the pure acoustic damping in a reliable and robust manner, and is applicable to transversal modes in non-compact thermoacoustic systems. The development, verification and validation of such a methodology defines the central objective of this paper, and is presented in the following sections.

1.3 Modeling Methodology

The methodology proposed to model and quantify vortical damping of transversal modes is based on the Helmholtz equation, which is given in conservation form by

$$i\omega \hat{p}_a + \gamma \bar{p} \nabla \cdot \hat{\mathbf{u}}_a = 0, \quad (13)$$

$$\bar{\rho} i\omega \hat{\mathbf{u}}_a + \nabla \hat{p}_a = \hat{\mathbf{F}}_{\hat{\mathbf{u}}_a}. \quad (14)$$

These equations yield irrotational velocity disturbance fields driven by pressure disturbance as the potential, and are thus purely acoustic quantities. Furthermore, this irrotationality implies that any damping rate computed by solving Eqns. 13-14 describes pure acoustics, too, which is precisely the desired quantity required for thermoacoustic stability assessments. The acoustic dissipation due to vortex shedding is modeled as a sink of momentum, while discarding the capturing of any hydrodynamic effects. Mathematically, this sink of momentum is modeled by linearly expanding the volumetric source term in Eqn. 14 to the first order, i.e.

$$\hat{\mathbf{F}}_{\hat{\mathbf{u}}_a} = \mathbf{D} \cdot \hat{\mathbf{u}}_a \cdot \delta(\mathbf{x} - \mathbf{x}_D). \quad (15)$$

The matrix \mathbf{D} is assumed to unfold into a 3×3 diagonal matrix with entries $\mathbf{D}(1, 1) = \zeta_x$, $\mathbf{D}(2, 2) = \zeta_r$, and $\mathbf{D}(3, 3) = \zeta_\theta$. These quantities can be interpreted as acoustic loss coefficients in an analogous manner as the ζ_{LF} coefficient occurring in vortical damping models [5] for low-frequency instabilities. The Dirac function in Eqn. 15 indicates that the damping term is only defined in the region (spatially described by x_D where dissipation physically occurs in the chamber (i.e. at the edge of the burner outlet, cf. Fig. 1d)), across which the loss strength can be assumed constant. This dissipation region can be qualitatively identified (cf. Fig. 1d) using Howe's equation for acoustic power absorption (period averaged) in free shear layers, i.e.

$$\hat{P}_a(\mathbf{x}) \propto |[\bar{\boldsymbol{\Omega}} \times \hat{\mathbf{u}} + \hat{\boldsymbol{\Omega}} \times \bar{\mathbf{u}}] \cdot \hat{\mathbf{u}}_a| \quad (16)$$

where $\hat{\mathbf{u}}$ is the total velocity disturbance field of Eqn. 10 and $\hat{\mathbf{u}}_a$ is the irrotational component, respectively. The evaluation of Howe's power dissipation field requires vorticity and velocity disturbance fields, which can be directly retrieved from LEE solutions at the frequencies of interest. The irrotational velocity field can be approximated using pressure disturbance of the LEE solution and the homogenous acoustic momentum equation in Eqn. 14 via $\mathbf{u}_a = (i\nabla\hat{p})/(\bar{\rho}\omega)$. Assuming that dissipation of acoustics due vortex-shedding physically occurs along the streamline of the mean flow allows to functionally connect the three coefficients in Eqn. 15, and reduce the number of unknown loss coefficients from three to one. The loss matrix becomes

$$\mathbf{D} = \zeta \cdot \mathbf{G} \cdot \delta(\mathbf{x} - \mathbf{x}_D), \quad (17)$$

where the entries of the 3×3 diagonal matrix are given by $\mathbf{G}(1, 1) = g_{x,SL}$, $\mathbf{G}(2, 2) = g_{r,SL}$, $\mathbf{G}(3, 3) = g_{\theta,SL}$, and represent geometrical functions that are straight-forwardly retrieved from the streamlines of the mean flow field at the identified sink region x_D . Discretization of Eqns. 13 – 14 is carried out using a standard FEM scheme [8], while replacing the momentum source by the damping model of Eqns. 15 and 17 yields the algebraic system

$$i\omega \mathbf{E}_a \hat{\phi}_a = (\mathbf{A}_a + \zeta \mathbf{A}_D) \hat{\phi}_a, \quad (18)$$

where the subscript a indicates the solutions' pure acoustic/irrotational nature. Matrix \mathbf{A}_D is the discrete result of the damping model given by Eqns. 15 and 17. The remaining task before the damping rate can be computed is the determination of the loss coefficient ζ . This is achieved by imposing an equality requirement between the reflection coefficient of the concerned configuration obtained from respective simulations of the full LEE (which includes the physics) and the HE (which includes the damping model). Specifically, the reflection coefficient defined as the ratio of leaving and entering traveling acoustic waves of concerned volume, denoted with reference to Fig. 2 below as $\mathbf{R}(\omega) = \frac{\hat{\mathbf{F}}}{\hat{\mathbf{G}}}$.

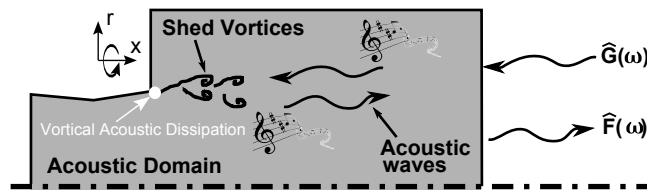


Figure 2: Characterization of an acoustic domain via a reflection coefficient

Using the Multi-Microphone-Method (MMM) to retrieve this reflection coefficient filters out any vortical disturbances present in the LEE solutions, and represents a unambiguous quantification of the pure acoustic damping due to the vortex shedding. Specifically, the MMM extracts the complex amplitudes of the traveling wave

components from the LEE pressure fields, which are then used to determine the desired reflection coefficients. Note that the MMM to obtain reflection coefficients of a system that includes transversal modes requires to account for the transversal variability of the traveling waves. Details on this procedure is omitted here due to space constraints, and can be retrieved from [10]. Thus, the value for ζ – which may be frequency dependent – that equates reflection coefficients of the LEE and HE system yields a quantitatively correct model of the pure acoustic damping due to vortex-shedding. Summarizingly, the determination of the loss coefficients occurs through the following steps:

1. Visualization of vortical dissipation region \hat{P}_a and identification of the sink location \mathbf{x}_D
2. Computation of the reflection coefficients \mathbf{R} over the frequency range of interest from LEE solutions
3. Determination of ζ values such that the reflection coefficient from 2. is reproduced by the HE model

Once the values of ζ are known across the concerned frequency band, Eqn. 18 can be solved for the eigenmodes of interest, which yields desired acoustics damping rate physically relevant for thermoacoustic stability assessments.

2. Test Case

This section presents the experimental combustor configuration used to validate the the above-proposed methodology. An atmospheric, isothermal operation point (air mass flow rate of $\dot{m} = 120\text{g/s}$ at $T = 293\text{K}$) of a premixed combustion test rig hosting a swirling mean flow field comprises the specific test case configuration. A schematic of the experimental setup is shown in Fig. 3, where the analysis domain is restricted to the chamber only. Note that detailed explanations of this setup along with experimental investigations and analyses of high-frequency thermoacoustic oscillations can be found in e.g. [1] and [2].

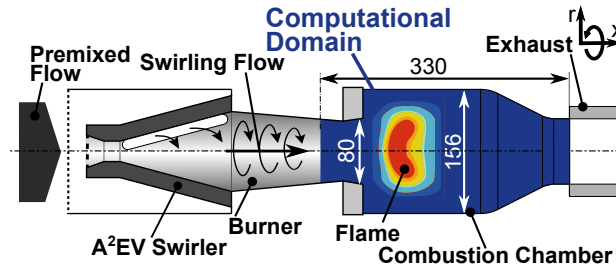


Figure 3: Schematic of experimental gas turbine combustion system

The swirling mean flow field, shown in Fig. 1b), can be viewed as representative of the flow conditions occurring in industrial (e.g. can type) gas turbine combustors. Furthermore, note the following remarks regarding the transferability of the isothermal test case to "real" combustor conditions with reactive flows: The region in which vortical damping occurs exhibits a relatively short axial extent as is shown by visualization of Howe's power dissipation term in Fig. 1d). This axial compactness justifies the non-consideration of a mean temperature distribution. In case a temperature distribution would be present, the vortical damping region x_D remains fully immersed within the isothermal part of the flow field, and would thus not "feel" any temperature gradient. Consequently, the loss coefficient ζ of a given flow field can be assumed as equal between isothermal cases and reactive counterparts.

Furthermore, the absence of combustion implies the absence of any thermoacoustic processes, leaving acoustic dissipation as the only mechanism determining the damping rate value. Thereby, optimal test case conditions are achieved, which is further ensured by nozzle-termination of the chamber: This enforces an axial increase of cut-on frequency value, which causes an attenuation of the first transversal mode towards a zero value at the outlet, and is thus, unaffected by any potential dissipation at the system outlet. Similarly, the smaller diameter of the burner tube creates independency of the inlet boundary condition at the first transversal chamber mode. Note that this axial attenuation equally occurs in systems with combustion, where the axial increase of the cut on frequency is caused by an increasing temperature/speed of sound [8]. Hence, the present isothermal nozzle configuration yields comparable first transversal mode shapes as occurring in reactive/thermoacoustic cases.

In the following, vortical damping of transversal modes within the test case configuration is modeled and quantified with the proposed methodology. Corresponding experimental benchmarks, i.e. oscillation frequencies and damping rates for two first transversal modes are available from previous work of the authors in [11].

3. Results

The first step of the proposed methodology requires the visualization of the dissipation region according to Howe's power dissipation relation. The respective normalized regions are shown for the first two transversal modes (T1 and T1L1) in Fig. 4a) and b), along with the local zones for the sink model. The size of this zone can be assumed invariant with frequency. The corresponding pressure mode shapes are shown in Fig. 4a) and b). The dotted perturbations after the burner edge clearly reveal the impact of hydrodynamic velocity perturbations. The FEM mesh along with the boundary condition required to compute the respective LEE (as well as subsequent HE) eigensolutions is shown in 4c).

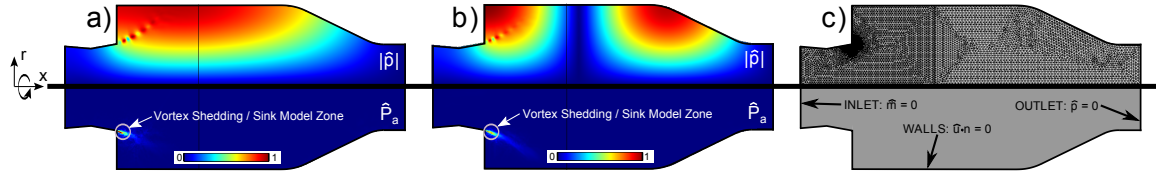


Figure 4: Normalized LEE pressure mode (top) and vorticity source/acoustic sink region (bottom) for T1 mode and b) T1L1 mode, c) FEM mesh and boundary conditions

Next, the reflection coefficient is computed. Note that this coefficient is not obtained from the LEE eigensolutions of the given configuration in Fig. 4. Rather, the Riemann invariants are extracted from (forced) field solutions (without the nozzle) of the LEE in Eqn. 9 for a prescribed set of real frequencies as a response to an external excitation. The selected frequency band is $f = (1200 : 35 : 1795) \text{ Hz}$, which includes the eigenfrequencies of the T1 and T1L1 modes in the test case combustor. The stabilization parameter (cf. Eqn. 9) is set to $\tau = 1$, which emerged as the minimum value that yields non-spurious solutions. Specific information regarding the obtainment procedure of the reflection coefficient is omitted due to space constraints, and one is referred to the literature [10]. The magnitude of the resulting reflection coefficient is displayed in Fig. 5a) and reveals a nearly constant behaviour across the concerned frequency range. The loss-coefficient ζ , which yields the reproduction of the LEE reflection coefficient through the HE model is shown in Fig. 5b).

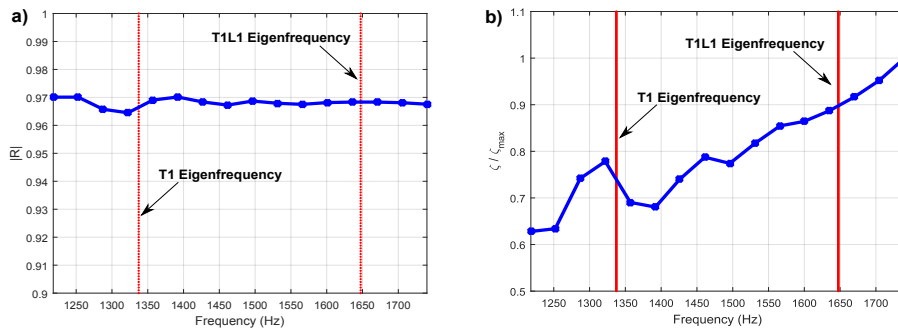


Figure 5: a) Reflection coefficient of LEE benchmark b) Matched loss coefficient

Finally, the complex eigenvalues of Eqn. 18 are computed for the T1 and T1L1 mode of the nozzle domain under consideration of the ζ distribution in Fig. 5b). The resulting damping rate values describe the pure acoustic damping due to vortex-shedding as desired, and are provided in Tab. 1. The table contains the measured counterparts of the damping rate and oscillations frequency, and reveals an accurate reproduction of the measurement benchmarks by the model. Furthermore, the imaginary part of eigenfrequency obtained by directly solving the LEE for its eigensolutions of the given combustor configuration – including acoustic and hydrodynamic contributions – are listed too, which reveals a significant deviation against the computed/measured pure acoustic counterparts, and clearly should not/cannot be used for any thermoacoustic stability assessment.

Conclusions

This paper presented a methodology to quantify the acoustic damping of transversal modes due to vortex-shedding in thermoacoustically non-compact gas turbine combustors. Specifically, can-type combustors con-

	$\alpha_{EXP}(rad/s)$	$\alpha_{HE}(rad/s)$	$\alpha_{LEE}(rad/s)$	$f_{EXP}(Hz)$	$f_{HE}(Hz)$	$f_{LEE}(Hz)$
T1	-15 ± 2	-16	-1.1	1312	1337	1336
T1L1	-25 ± 3	-24	-1.5	1620	1647	1650

Table 1: Measured and calculated growth rates and oscillation frequencies [11]

taining a swirling flow field were considered as the technical target application. The computed damping rates present a substantial ingredient for the numerical assessment of a combustors's thermoacoustic stability behaviour. The computation of a direct eigensolution of the Linearized Euler Equations (with an underlying mean flow that contains strong shear layers) to retrieve the acoustic damping rates is impossible as the LEE describe acoustic as well as also hydrodynamic disturbance contributions. Instead, one has to perform computations that exclusively solve for acoustic disturbances. This is achieved by the presented methodology as it based on the Helmholtz Equation including a sink function of acoustic momentum to model the vortical damping effect on the acoustics. This sink is locally defined in accordance with the zone of dissipation that is given by Howe's analytical dissipation equation. Assuming that dissipation occurs along the streamline defines this sink as a function of the local acoustic velocity and a loss coefficient. This loss coefficient is determined by an imposed equality requirement based on transversal acoustic reflection coefficients, which can be effectively retrieved from forced solutions of the Linearized Euler Equations. The desired acoustic damping rates are then computed by solving for the Helmholtz Equation including the sink term with loss-coefficients for the acoustic modes of interest. An isothermal and atmospheric validation was carried out using a test case of a swirl-stabilized combustor configuration, which yielded a simplified, but transferable flow conditions as occurring in technically relevant industrial gas turbine combustors. The first two transversal modes (T1 and T1L1) served as target to determine respective damping rates for comparison against readily available counterparts from experimental measurements. The experimental benchmarks were successfully reproduced, which validated the proposed methodology, and granted it eligible to be used for computing acoustic damping rates relevant for the numerical assessment of non-compact, high-frequency thermoacoustic instabilities.

References

1. Schwing, J., Noiray, N., and Sattelmayer, T., 2011. "Interaction of Vortex Shedding and Transverse High-Frequency Pressure Oscillations in a Tubular Combustion Chamber". *ASME GT2011-45246*, June 6-10, 2011, Vancouver, British Columbia, Canada.
2. Berger, F., Hummel, T., Hertweck, M., Schuermans, B., and Sattelmayer, T., 2016. "High-Frequency Thermoacoustic Modulation Mechanisms in Swirl-Stabilized Gas Turbine Combustors, Part I: Experimental Investigation of Local Flame Response". *Journal of Engineering for Gas Turbines and Power*, **139**(7), pp. 071501–071501–9.
3. M.S.Howe, 1979. "On the Theory of Unsteady High Reynolds Number Flow Through a Circular Aperture". *Proceedings of the Royal Society A*, **366**, pp. 205–223.
4. Lieuwen, T., 2012. *Unsteady Combustor Physics*. Cambridge University Press.
5. Rienstra, S., and Hirschberg, A., 2016. *An Introduction to Acoustics*.
6. Schuermans, B., Bellucci, V., and Paschereit, C. O., 2003. "Thermoacoustic Modeling and Control of Multi Burner Combustion Systems". *ASME GT2005-38688*, June 16-19, Atlanta, GA, USA.
7. Schuermans, B., Bothien, M. R., Maurer, M., and Bunkute, B., 2015. "Combined Acoustic Damping-Cooling System for Operational Flexibility of GT26/24 Reheat Combustors". *ASME GT2015-42287*, June 15-19, Montreal, Canada.
8. Hummel, T., Berger, F., Hertweck, M., Schuermans, B., and Sattelmayer, T., 2016. "High-Frequency Thermoacoustic Modulation Mechanisms in Swirl-Stabilized Gas Turbine Combustors, Part II: Modeling and Analysis". *Journal of Engineering for Gas Turbines and Power*, **139**(7), pp. 071502–071502–10.
9. Schulze, M., Hummel, T., Klarmann, N., Berger, F., Schuermans, B., and Sattelmayer, T., 2016. "Linearized Euler Equations for the Prediction of Linear High-Frequency Stability in Gas Turbine Combustors". *ASME Turbo Expo 2016 GT2016-57913*, June 13-17, Seoul, South Korea.
10. Kathan, R., 2013. "Verlustmechanismen in Raketenbrennkammern". *PhD Thesis, Lehrstuhl f. Thermodynamik, Technische Universität München*, www.td.mw.tum.de.
11. Hummel, T., Berger, F., Schuermans, B., and Sattelmayer, T., 2016. "Theory and modeling of non-degenerate transversal thermoacoustic limit cycle oscillations". In *Proceedings of the International Symposium on Thermoacoustic Instabilities in Gas Turbines and Rocket Engines: Industry meets Academia*, TUM, LS für Thermodynamik / IAS.